Measurement of the transverse coherence of a VUV Free Electron Laser

Rasmus Ischebeck, Manfred Tonutti (RWTH Aachen), Josef Feldhaus, Christopher Gerth*,
Evgeni Saldin, Evgeni Schneidmiller, Kai Tiedtke, Rolf Treusch (DESY),
Peter Schmüser (Universität Hamburg and DESY) Mikhail Yurkov (JINR Dubna),

ABSTRACT

The transverse coherence is important for many applications of a free electron laser (FEL). It depends on the inner structure of the electron bunch in the undulator, which is difficult to measure. It is therefore essential to determine the coherence properties of the FEL radiation directly.

The coherence of the vacuum ultraviolet FEL at the TESLA Test Facility has been measured by recording the diffraction pattern of a double slit and measuring the visibility of the interference fringes. The experimental near field diffraction pattern is compared with a numerical model, taking into account the formation of the FEL radiation, the Fresnel diffraction in the near field zone and effects of the experimental set-up.

Diffraction patterns have been recorded for various effective undulator lengths to measure the evolution of the transverse coherence along the undulator. This is compared to the expected evolution of the transverse radiation modes.

DIFFRACTION AT A DOUBLE SLIT

The intensity in the far field (or *Fraunhofer*) diffraction pattern of a double slit is described by the well-known equation

$$I(x) = \left(\frac{\sin(\pi w x/(\lambda L))}{\pi w x/(\lambda L)}\right)^2 \left[1 + \mathcal{C}\cos\left(\frac{2\pi d}{\lambda L}x\right)\right] \quad (1)$$

where w is the width and d the separation of the slits, L the distance to the observation plane, λ the wavelength and $\mathcal{C}$ the transverse coherence between the two slits. A homogeneous intensity distribution before the double slits and a sufficiently large longitudinal coherence are assumed. The visibility of the diffraction fringes

$$\mathcal{V} = \frac{I_{\max} - I_{\min}}{I_{\max} + I_{\min}} \quad (2)$$

is equal to the coherence $\mathcal{C}$.

If the far field condition $L \gg \pi d^2/\lambda$ is not fulfilled, Fresnel theory has to be employed. Generally, the diffraction pattern can be computed only by numerical methods. However, at intermediate distances where $\pi w^2/\lambda \ll L < \pi d^2/\lambda$, the diffraction patterns of the single slits may be computed in the far field approximation. This is the case for the present setup.

A transverse coherence $\mathcal{C}$ between the wave fronts at the two slits is assumed. The patterns of the two slits are labeled $I_1(x) = |\tilde{E}_1(x)|^2$ and $I_2(x) = |\tilde{E}_2(x)|^2$, where $\tilde{E}$ is the complex amplitude of the radiation field. If the fields are added coherently one obtains an intensity distribution (shown in Fig. 1):

$$I(x) = \mathcal{S}(x)\left[1 + \mathcal{C}\cdot\mathcal{W}(x)\cos\left(\frac{2\pi d}{\lambda L}x\right)\right] \quad (3)$$

where the amplitude is

$$\mathcal{S}(x) = I_1(x) + I_2(x) \quad (4)$$

The intensities in the extrema are

$$I_\pm(x) = (\tilde{E}_1(x) \pm \tilde{E}_2(x))^2 \quad (5)$$

and a position-dependent visibility factor can be calculated

$$\mathcal{W}(x) = \frac{I_+(x) - I_-(x)}{I_+(x) + I_-(x)} \quad (6)$$

EXPERIMENTAL SETUP

The free electron laser installed at the TESLA Test Facility (TTF FEL) uses a superconducting linear accelerator to produce an electron beam with a particle energy of 300 MeV. During the passage of this beam through a permanent magnet undulator, electromagnetic radiation with a wavelength around 100 nm is emitted. The interaction between electrons and the photon field results in the development of a micro-structure in the electron bunch. A large number of electrons emit radiation coherently and the radiation intensity grows exponentially with the longitudinal position z in the undulator.

A double slit interference measurement allows a straightforward determination of the transverse coherence [1]. Because of the high peak intensity of the FEL beam, close to

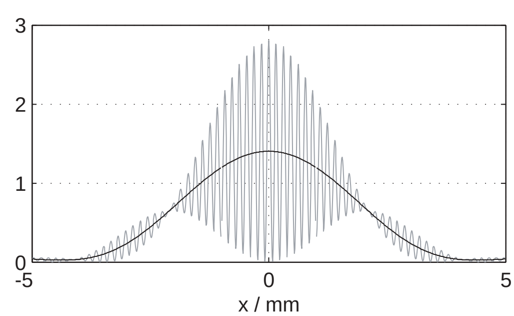

Figure 1: Formation of a double slit diffraction pattern in the near field. Amplitude modulation (black line) and double slit diffraction pattern (grey line)

* current address: ASTeC, Daresbury Laboratory

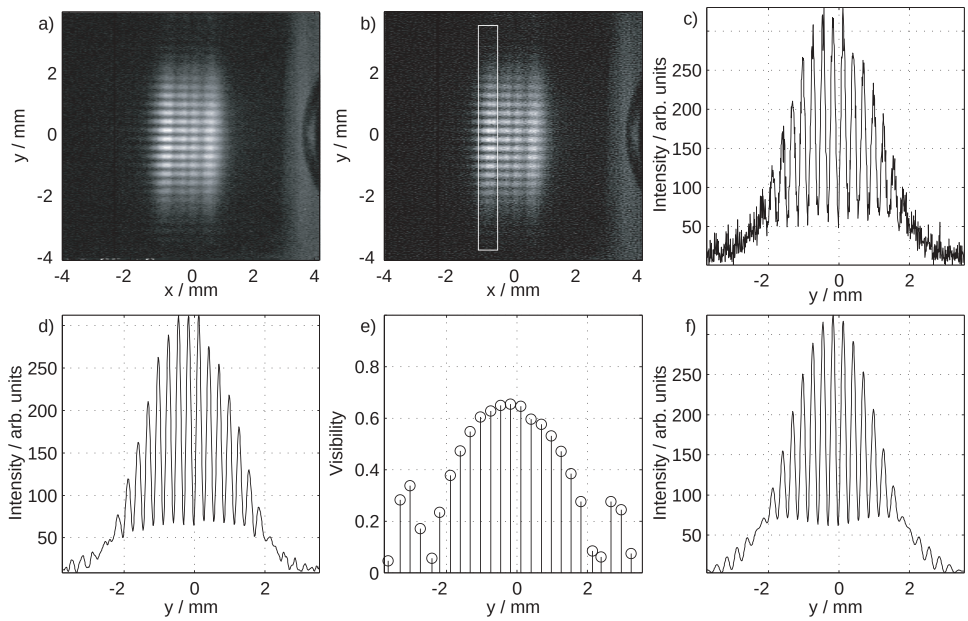

Figure 2: Analysis of the diffraction images: a) measured image, b) deconvoluted and linearized image, c) projection of the diffraction pattern, d) smoothed projection, e) visibility of the diffraction fringes, f) fit to the intensity distribution.

the destruction limit of most detector materials, a two-stage detection mechanism for the radiation has been employed. The diffraction pattern forms on a fluorescent Ce:YAG crystal, 3.1 m behind the slits. The fluorescence light is imaged onto a cooled CCD detector. Since the space behind the fluorescent crystal is occupied by another detector, the imaging is done with a tilted lens set-up. A commercial lens system (Nikkor 85mm f/2.8D), corrected for the complete visible spectrum, provides a good focusing over the complete crystal.

Slit pairs separated by 0.5, 1 and 2 mm and with a slit width of 100 μm were used. The diffraction patterns from different slit separations show the dependency of the transverse coherence on the distance. The diffraction fringes of the horizontal double slits are clearly visible (see Fig. 2 a), their spacing is inversely proportional to the separation of the slits. An intensity variation is also visible along the direction of the slits, i.e. the horizontal axis. Two absolute maxima near the end of the slit and two smaller relative maxima in the middle are visible. This pattern is due to the finite slit length.

ANALYSIS

The images have been corrected for the limited resolution of the optical system by deconvolution with the measured point spread function. The Lucy-Richardson algorithm [2, 3] has been used to this effect. The transverse coherence has been extracted from the corrected images using two analysis methods (see Fig. 2 b … f): Firstly, the visibility of the diffraction fringes in the middle of the image was directly determined. Secondly, a function according to Eq. (3) has been fitted to the measurements.

For the first method, a central part of the diffraction pattern has been projected along the direction of the slits, resulting in a one-dimensional distribution. The visibility of the diffraction fringes can be calculated from the extrema of this curve, according to equation (2). However, the image recorded by the CCD chip is affected by read-out noise. Taking the pixels with the highest and lowest contents as maxima and minima respectively overestimates the modulation, as the maxima and minima of the diffraction pattern extend over several pixels: the highest pixel within a maximum overestimates the peak, the lowest pixel within a minimum underestimates the latter. It is therefore necessary to reduce the noise by smoothing the curve before the extrema are determined.

This has been done by applying a Butterworth filter, which reduces the pixel noise without degrading the modulation in the observed pattern. For the diffraction pattern at 1 mm slit separation, for example, the selected filter has a transmission of more than 96% for the diffraction pattern, while the pixel noise is reduced to 17%. The visibility of the diffraction fringes has been determined from this smoothed curve according to Eq. (2). The central visibility is used as a measure for the coherence.

For the second method, the algorithm used to to fit the intensity function according to Eq. (3) to the data is based on the *reflective Newton* method on *trust-regions* [4]. For the present case of seven optimisation parameters, the trust-region reflective Newton algorithm is superior to the commonly used simplex search method. The fit was performed first for the averaged diffraction pattern of 100 FEL bunches. The parameters determined from this fit were then used as starting parameters for the fit of the individual bunches.

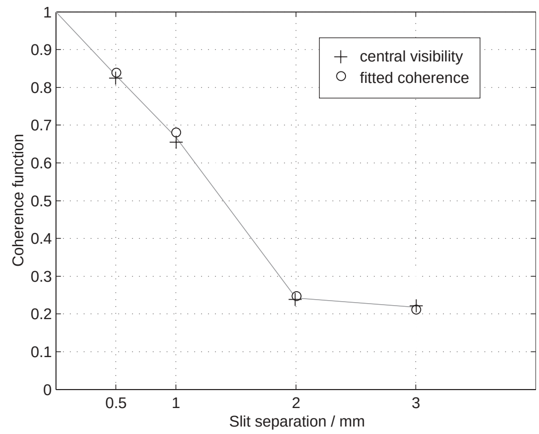

Figure 3: Measured coherence function of the FEL as a function of transverse distance.

RESULTS

For the present measurements, the TTF FEL was running reliably with a bunch charge of 1.95 nC. The FEL process was saturated, i.e. maximum output power was reached. This was confirmed by observing the bunch-to-bunch fluctuations of the FEL pulse energy: saturation leads to a smaller variance in the otherwise purely stochastic FEL process. The wavelength of the radiation was measured with a spectrometer to be 100 nm. The middle of the two slits was aligned with respect to the centre of the beam.

The results of both analysis methods presented in the previous section are summarized in Fig. 3. The systematic uncertainties of the measurements have been estimated from the analysis of simulated images [5]. Statistic uncertainties have been obtained by analyzing 100 images.

The radiation in an FEL can be decomposed in its transverse modes [6]. The fundamental mode TEM_{00} grows fastest because it has the best overlap with the electron beam. Its intensity surpasses quickly all other modes, resulting in a growing transverse coherence. Saturation in the FEL amplification process occurs first for the fundamental mode, whereas the power in the other modes is still growing. Since the different modes have a random phase distribution, their contribution to the overall intensity reduces the transverse coherence of the beam.

To measure the evolution of the coherence as a function of the FEL amplification process, i.e. as a function of the longitudinal (z) position in the undulator, the electron beam was deflected from the ideal orbit by steering magnets. These separate the electron and photon beams by approximately 1 mm, which is sufficient to inhibit the FEL exponential growth of the radiation power after the position of the magnet. Effective undulator lengths between $z = 9.37$ m and 13.5 m have been measured.

For each effective undulator length, horizontal double slits with separations of 0.5, 1 and 2 mm have been inserted into the FEL beam. In the present measurements, the maximum of the coherence is observed at approximately 11 m as shown in Fig. 4 a. The transverse coherence for a slit separation of 1 mm increases up to a value of 0.9. Measurements with the microchannel plate detector [7] show that for this undulator length, saturation occurs. This can be seen from both the pulse energy and its variance: the energy growth rate decreases and the variance is reduced (see Fig. 4 b). A further increase of the effective undulator length beyond saturation degrades the coherence of the photon bunch: for the full undulator length, it is reduced to a value of 0.7 for a transverse distance of 1 mm.

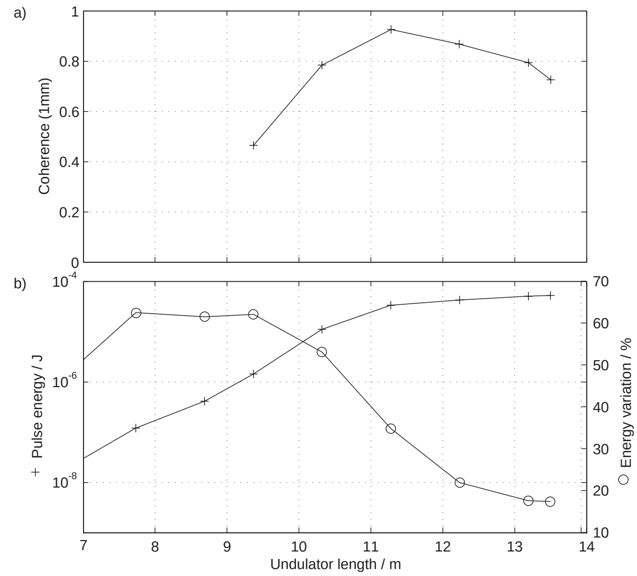

Figure 4: a) Evolution of the coherence along the undulator. The value of the coherence function at 1 mm separation is shown as a function of z position. b) The total energy (+) of the photon pulse and the energy fluctuations (o) indicate the onset of saturation at a length of 11 m.

REFERENCES

[1] R. Ischebeck et al. Study of the transverse coherence at the TTF free electron laser. *NIM A*, 507:175–180, 2003.

[2] L.B. Lucy. An iterative technique for the rectification of observed distributions. *The Astronomical Journal*, page 745ff., June 1974.

[3] William Hadley Richardson. Bayesin-based iterative method of image restoration. *Journal of the Optical Society of America*, page 55ff., January 1972.

[4] T.F. Coleman and Yuying Li. An interior trust region approach for nonlinear minimization subject to bounds. *SIAM J. Optimization*, 6(2):418–445, 1996.

[5] R. Ischebeck et al. *to be published in: PR ST-AB.*

[6] E.L. Saldin, E.A. Schneidmiller, and M.V. Yurkov. *The Physics of Free Electron Lasers*. Springer, 2000.

[7] V. Ayvazyan et al. A new powerful source for coherent VUV radiation: Demonstration of exponential growth and saturation at the TTF free-electron laser. *European Physical Journal D*, 20:149–156, 2002.